

## EFFECT OF STRESSES ACTING ON IMPELLER BLADES

by

**Ismail BOGREKCI<sup>a\*</sup>, Pinar DEMIRCIOGLU<sup>a,b</sup>, Berkay SERT<sup>c</sup>,  
Ahmet GOGEBAKAN<sup>c</sup>, and Mujtaba ABBAKAR<sup>c</sup>**

<sup>a</sup> Graduate School of Natural Applied Science, Department of Mechanical Engineering,  
University of Aydin Adnan Menderes University, Aydin, Turkiye

<sup>b</sup> TUM School of Engineering and Design, Institute of Materials Science,  
Technical University of Munich, Garching, Germany

<sup>c</sup> HAUS Centrifuge Technology R&D Center, Aydin, Turkiye

Original scientific paper

<https://doi.org/10.2298/TSCI2304113B>

*This paper examines the impact of temperature, pressure, and blade thickness on the stresses experienced by impeller blades during operation. The impeller is subject to a range of stresses arising from thermal, fluid, and mechanical factors that can cause deformation if they exceed certain thresholds. The study focuses on an impeller supplied by HAUS Centrifuge Technologies, which suffered damage while operating at 33000 rpm. Six blade thickness offsets, ranging from 0.05 mm to 0.15 mm, were analyzed structurally, and the Von-Mises stresses were compared to the impeller material yield strength. The impeller with the lowest stress, at 197.43 MPa, was chosen for fluid-structure interaction analysis. The impeller was then manufactured and tested for performance using ISO 5389 standard in HAUS test facility. The CFD results indicated that the polytropic efficiency of the thickened impeller increased to 86.57%, compared to the original impeller polytropic efficiency of 75.8%. However, the volumetric flow decreased from 4211.3 m<sup>3</sup> per hour to 3658.3 m<sup>3</sup> per hour when using “the thicker impeller”. The data collected supports the conclusion that an increase in blade thickness can help to reduce the stresses acting on the blade.*

**Key words:** *blade thickness, CFD, fluid-structure interaction, impeller, Von-Mises stress, polytropic efficiency*

### Introduction

During operation, the compressor draws in air through the inlet cover, which then passes through the impeller. The process of pressurizing the air subjects the impeller to various types of stresses, including thermal, fluid, and centrifugal forces. When these stresses exceed a certain threshold, they can cause the impeller blades to deform or even fracture, as illustrated in fig. 1. As such, a thorough understanding of the stresses experienced by the impeller is crucial for ensuring the reliable and efficient operation of the turbo compressor.

The cost of manufacturing impellers is significant, and once an impeller is damaged, it cannot be repaired. Therefore, it is crucial to calculate and choose the impeller design parameters carefully prior to production. To mitigate the risk of manufacturing suboptimal impellers, computer aided engineering (CAE) software is employed to analyze and optimize impeller designs. Structural and fluid analyses can be conducted using CAE software to identify high-stress areas on the impeller and prevent the production of suboptimal designs [1]. By us-

\* Corresponding author, e-mail: [ibogrekci@adu.edu.tr](mailto:ibogrekci@adu.edu.tr)



**Figure 1. Fracture on impeller blade (HAUS Turbo blower impeller)**

ing CAE software, manufacturers can ensure the production of high-quality impellers that meet their intended specifications while minimizing the risk of costly and irreparable damage.

The Coriolis and centrifugal forces exerted by the impeller can be analyzed through the use of fluid-structure interaction (FSI) analysis, which involves the interaction between fluid-flow and a solid structure. There are two main methods of conducting FSI analysis: one-way coupling and two-way coupling analysis. In a one-way coupling analysis, CFD analysis is conducted first, and the results are subsequently imported into the structural analysis module. In contrast, a two-way coupling analysis begins with the structural analysis, and the results are then transferred to a CFD module. In a study conducted by Berna *et al.* [2] in 2011, a comparison was made between the one-way coupling and two-way coupling methods. The FSI analysis is a valuable tool for assessing impeller performance and identifying the forces that impact its structural integrity.

Recent research has examined the impact of FSI on rotational forces. These studies have shown that fluid pressures can have a significant effect on the Von-Mises stress, which is a key determinant of a material's ability to withstand fracture or yield [2, 3]. By understanding the effects of FSI on rotational forces, researchers can identify potential sources of stress and develop strategies for optimizing impeller designs to minimize these impacts.

As noted previously, there are two methods for conducting an FSI simulation. In a one-way coupling analysis, pressure forces can have significant implications for impeller structural strength, lifespan, and stability, as documented in a number of studies [4-11]. Conversely, in a two-way coupling analysis, the structural deformation of impeller blades can impact aerodynamic stresses within the impeller, as described in other research [5, 9, 10]. Consequently, blade thickness is a key design parameter that must be chosen carefully, as it can have a substantial impact on the overall efficiency and performance of the turbo blower, as highlighted in previous investigations [12].

### **Material and methodology**

The primary objective of this investigation is to evaluate the influence of blade thickness on Von-Mises stresses. The choice of material for the impeller is a critical aspect as it directly affects the strength of the impeller blades [13]. In this study, an aluminum alloy (AL T6 7075) impeller with a yield strength of around 490 MPa was employed. Six distinct impeller models were examined, each with varying blade thicknesses as presented in tab. 1. Furthermore, the weight of the impellers was considered, as it can impact the balance of the magnetic bearings. A structural analysis was performed on all six models to determine the impeller with the lowest Von-Mises stress. For the FSI analysis, the original impeller and the impeller with the least Von-Mises stress were employed for comparison purposes.

In order to conduct the analysis, the ANSYS software was utilized to perform a steady-state pressure-based analysis based on the Navier-Stokes method, which employs a finite volume discretization method [14]. A mesh size of 0.4 mm was employed for the blade tips, while the hub, shroud, inlet, and outlet had mesh sizing of 5 mm, 5 mm, 10 mm, and 5 mm, respectively. In addition, an inflation layer consisting of 8 layers and a total layer thickness of 0.2 mm was added to the blades, hub, and shroud. To simplify the mesh and save

time during the structural analysis, the impeller was divided into various sections, with a face mesh size of 0.4 mm for the blades and 5mm for the remaining sections.

**Table 1. Impeller blade thickness**

Impeller blade thickness			Impeller blade thickness		
Blade offset [mm]	Weight gain [g]	Total weight [g]	Blade offset [mm]	Weight gain [g]	Total weight [g]
Original	–	2135.5	0.1	26.75	2162.3
0.05	12.863	2148.4	0.125	34.82	2170.4
0.075	20.78	2156.3	0.15	42.06	2177.6

The impeller provided by HAUS can operate at a maximum rotational velocity of 33000 rpm with a pressure rise of 1 bar and ambient temperature 40 °C. These operating conditions were replicated for the FSI analysis. For the CFD analysis, a shear-stress transport turbulence model was employed, along with an automatic wall function and a heat transfer model of total energy as domain boundary conditions. A residual target of  $10^{-6}$  was also set for the analysis. The same boundary conditions were applied for the structural analysis of the impeller, fig. 2.

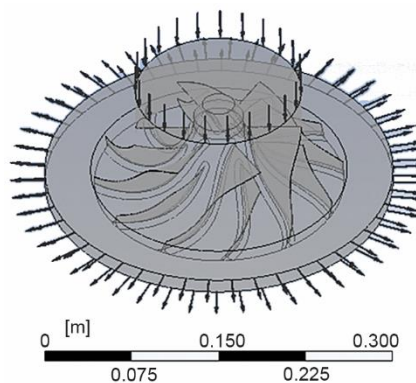


**Figure 2. Impeller fluid domain**

## Results and discussion

### Initial selection of impeller

Based on the results obtained from the initial static structural analysis, it can be inferred that the impeller Von-Mises stresses were well within the material yield stress limit. Additionally, as depicted in fig. 3, it is evident that the 0.1 mm offset exhibited the lowest stress magnitude.

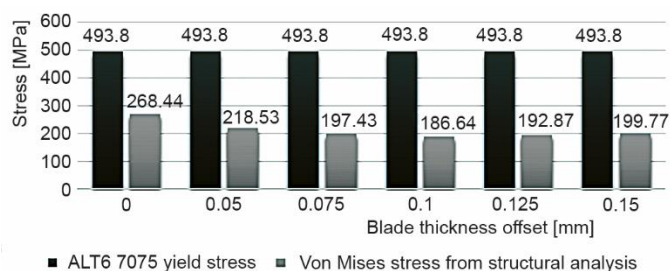


**Figure 3. Von-Mises stress vs. yield stress comparison of original and thickened impeller**

### The CFD results

The polytropic efficiency can be calculated using the polytropic exponent  $k$ . The value of the polytropic exponent  $k$  is dependent on the pressure ratio and temperature ratio. The formulas for these calculations were taken from the ISO 5389 standards [8]:

$$\eta_p = \frac{n(k-1)}{k(n-1)} \quad (1)$$

where  $n$  is the isentropic exponent. The value of the isentropic exponent for ideal gases is approximately 1.4 according to the ISO 5389 standards:

$$n = \frac{\ln\left(\frac{P_2}{P_1}\right)}{\ln\left(\frac{P_2}{P_1}\right) - \ln\left(\frac{T_2}{T_1}\right)} \quad (2)$$

The polytropic efficiency, calculated from the CFD results, pertains solely to the impeller and not to the compressor stage as a whole. Typically, the pressure ratio is influenced

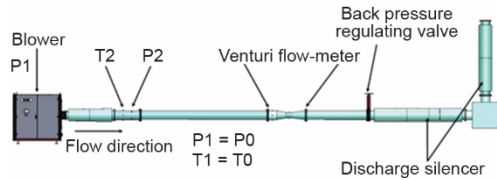


Figure 4. The HAUS turbo blower test bench

by the impeller rotational speed, and therefore, differences in pressure ratio are negligible. Research has shown that polytropic efficiency increases as the pressure ratio decreases. Additionally, the thickened impeller temperature ratio was lower than that of the original impeller, leading to a decrease in discharge temperature and a 4.49% increase in polytropic efficiency. Studies have demonstrated that high temperatures induce greater stresses on the impeller.

Another important factor that was of concern was the volume flow. Since the impeller blades thickened, it was assumed that there would be a decrease in volume flow. The results from the CFD analysis show a slight decrease in the volume flow.

The HAUS turbo blower was used to run performance tests on the impeller, fig. 4. The turbo blower and the discharge pipes were set up according to the ISO 5167 standards. During the performance test of the impellers, it was observed that there was a slight increase in the polytropic efficiency during the compression stage, tabs. 4 and 5. Similar to the CFD results, we can see that there is a decrease in the volume flow. However, the decrease is much more significant for the whole compression stage compared to the CFD results, which only consists of the domain near the impeller.

Tables 2 and 3 show the CFD results of both the impellers. The maximum and minimum discharge pressures, 1.8 bar and 1.25 bar, respectively, were used as boundary conditions for the analysis. The general trend that can be observed from these graphs is that the original impeller has a higher volume flow but a lower polytropic efficiency. The decrease in volume flow is due to the fact that geometrically increasing the thickness of the blades decreases the fluid passage area between the blades. The polytropic efficiency of the thicker impeller was higher than the original when calculated from eq. (1).

The data collected from the test bench from tabs. 4 and 5 shows a similar pattern to that of the CFD analysis. The temperature ratios from all the tables are very similar even though the CFD setup had different boundary conditions. The discharge pressure was the main determining factor for the polytropic efficiency and volume flow.

According to eq. (1), the temperature ratio is also a factor that determines the polytropic efficiency. However, from the tables there is not too much difference between temperature ratios. At lower rotational speeds and pressure ratios, the impeller is unable to reach 2 bar

**Table 2. The CFD results of original impeller**

Original impeller				
Boundary conditions				
Rotational velocity	27000 rpm	27000 rpm	33000 rpm	33000 rpm
Pressure inlet	1.00 bar	1.00 bar	1.00 bar	1.00 bar
Pressure outlet	2.00 bar	1.25 bar	2.00 bar	1.25 bar
CFD results				
$P1$	106000 Pa	101200 Pa	101300 Pa	101500 Pa
$P2$	174900 Pa	125000 Pa	200100 Pa	125100 Pa
Mass-flow	0.144 kg/s	2.139 kg/s	1.433 kg/s	2.709 kg/s
$P2-P1$	68900 Pa	23800 Pa	98800 Pa	23600 Pa
$P2-P1$	689 mbar	238 mbar	988 mbar	236 mbar
$P2/P1$	1.65	1.235	1.98	1.23
$T1$	328.10 K	310.90 K	313.70 K	305.80 K
$T2$	396.30 K	344.60 K	393.30 K	351.40 K
$T2/T1$	1.208	1.108	1.254	1.149
Polytropic efficiency, $\eta$	74.00%	57.39%	84.61%	41.28%
Volume flow, $Q$	423.2 m <sup>3</sup> /h	6286.0 m <sup>3</sup> /h	4211.3 m <sup>3</sup> /h	7961.1 m <sup>3</sup> /h

**Table 3. The CFD results of thickened impeller**

Thickened impeller				
Boundary conditions				
Rotational velocity	27000 rpm	27000 rpm	33000 rpm	33000 rpm
Pressure inlet	1.00 bar	1.00 bar	1.00 bar	1.00 bar
Pressure outlet	2.00 bar	1.25 bar	2.00 bar	1.25 bar
CFD results				
$P1$	113400 Pa	101200 Pa	101400 Pa	101300 Pa
$P2$	192000 Pa	125000 Pa	200100 Pa	125100 Pa
Mass-flow	0.00 kg/s	1.839 kg/s	1.245 kg/s	2.558 kg/s
$P2-P1$	78600 Pa	23800 Pa	98700 Pa	23800 Pa
$P2-P1$	786 mbar	238 mbar	987.000 mbar	238.000 mbar
$P2-P1$	1.693	1.235	1.973	1.235
$T1$	319.70 K	310.50 K	315.00 K	306.90 K
$T2$	382.30 K	348.30 K	393.00 K	352.00 K
$T2/T1$	1.196	1.122	1.248	1.147
Polytropic efficiency, $\eta$	82.92%	51.10%	86.57%	42.29%
Volume flow, $Q$	0.000 m <sup>3</sup> /h	5404.4 m <sup>3</sup> /h	3658.8 m <sup>3</sup> /h	7517.4 m <sup>3</sup> /h

**Table 4. Test bench results of original impeller**

Original impeller				
Rotational velocity	27000 rpm	27000 rpm	33000 rpm	33000 rpm
$P1$	101797.3 Pa	101850.9 Pa	102004.7 Pa	101863.4 Pa
$P2$	176267.3 Pa	120300.9 Pa	191804.7 Pa	125763.4 Pa
Mass-flow	0.893 kg/s	2.139 kg/s	2.317 kg/s	2.545 kg/s
$P2-P1$	74470.0 Pa	18450.0 Pa	89800.0 Pa	23900.0 Pa
$P2-P1$	744.7 mbar	184.5 mbar	898.0 mbar	239.0 mbar
$P2-P1$	1.732	1.181	1.88	1.235
$T1$	288.35 K	287.05 K	287.35 K	290.35 K
$T2$	351.33 K	326.19 K	364.52 K	351.01 K
$T2/T1$	1.218	1.136	1.269	1.209
Polytropic efficiency, $\eta$	79.40%	37.20%	75.80%	31.70%
Volume flow, $Q$	1844.0 m <sup>3</sup> /h	6003.4 m <sup>3</sup> /h	4556.0 m <sup>3</sup> /h	7352.9 m <sup>3</sup> /h

**Table 5. Test bench results of thickened impeller**

Thickened impeller				
Rotational velocity	27000 rpm	27000 rpm	33000 rpm	33000 rpm
$P1$	100513.9 Pa	100499.6 Pa	100841.2 Pa	101089.6 Pa
$P2$	172413.9 Pa	123429.6 Pa	201671.2 Pa	122649.6 Pa
Mass-flow	1.075 kg/s	1.802 kg/s	1.680 kg/s	2.282 kg/s
$P2-P1$	71900.0 Pa	22930.0 Pa	100830.0 Pa	21560.0 Pa
$P2-P1$	719.0 mbar	229.3 mbar	1008.3 mbar	215.6 mbar
$P2-P1$	1.715	1.228	2	1.213
$T1$	286.75 K	287.75 K	286.75 K	286.85 K
$T2$	368.53 K	341.15 K	368.53 K	345.80 K
$T2/T1$	1.285	1.186	1.285	1.206
Polytropic efficiency, $\eta$	83.10%	34.50%	78.90%	29.60%
Volume flow, $Q$	3175.0 m <sup>3</sup> /h	5157.0 m <sup>3</sup> /h	3175.0 m <sup>3</sup> /h	6660.4 m <sup>3</sup> /h

at the discharge. The CFD results from tab. 3 shows the volumetric flow to be zero. This is because at 27000 rpm and 2 bar, the impeller reached its surge point. At the surge point the back pressure is greater than the discharge pressure from the impeller therefore having a volumetric flow of zero.

*The FSI results*

Based on the FSI results, the original impeller appears to have reached its elastic limit. The Von-Mises stress of the impeller, fig. 5, has a maximum value of 577.95 MPa, surpassing the yield stress of AL T6 7075 (*i.e.*, 493 MPa), as stated previously. Notably, the fracture point observed in fig. 1 corresponds closely to the area where the impeller may experience the highest stress, as depicted in fig. 5. The total deformation of the original impeller was recorded at a maximum value of 1.3 mm. However, thickening the blade was found to reduce the overall stress on the blades, despite the maximum stress point located at the blade center, rather than the tip near the leading edge [15]. On the other hand, the maximum Von-Mises stress acting on the thickened impeller is 208.64 MPa. This value is significantly less than the material, which has a yield stress of 493 MPa. Figure 6 shows a drop from 1.3 mm to 0.9 mm in the total deformation in the blades of the impellers.

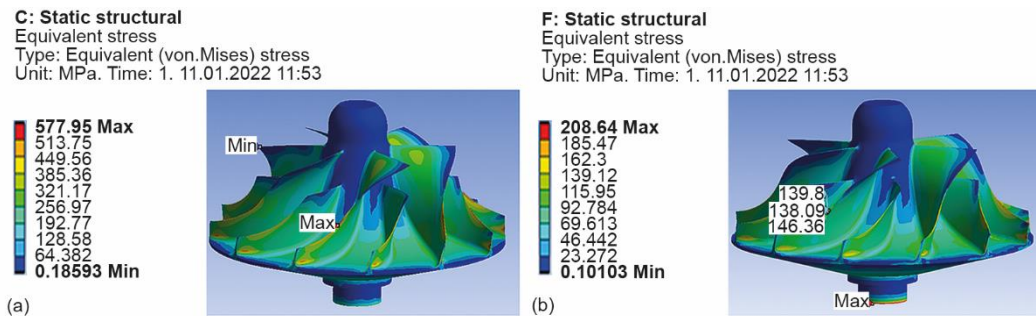


**Figure 5. Von-Mises stresses (a) original impeller and (b) thickened impeller**

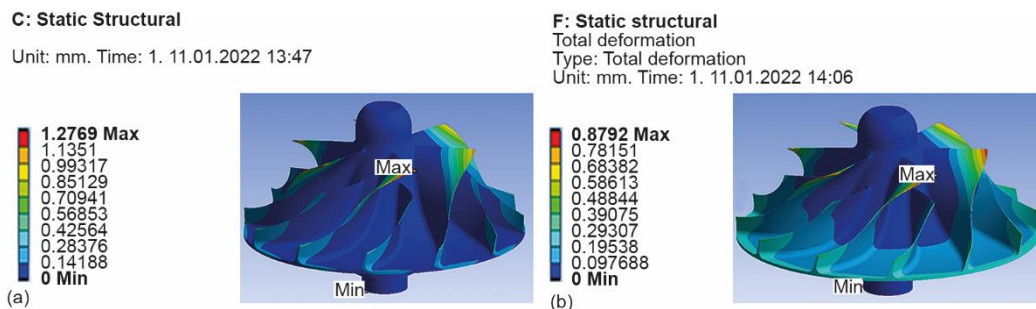


**Figure 6. Total deformation (a) original impeller and (b) thickened impeller**

*Performance data of test site*

Both impellers were manufactured at the HAUS factory and subjected to performance tests using the HAUS turbo blower XMP122, as per the ISO 5167 standards [7]. The resulting performance map allowed for a comparative analysis of the impellers' performance. The original impeller exhibited a marginally wider volume flow operating range than the thickened impeller. Specifically, at 33000 rpm, the thickened impeller failed to attain 1200 mbar prior to reaching the surge point, while the original impeller maintained operation just above 1200 mbar before reaching the surge point. The surge line displayed in fig. 7 un-

derwent a shift, and the volume flow capacity of the thickened impeller reduced to that of the original impeller.

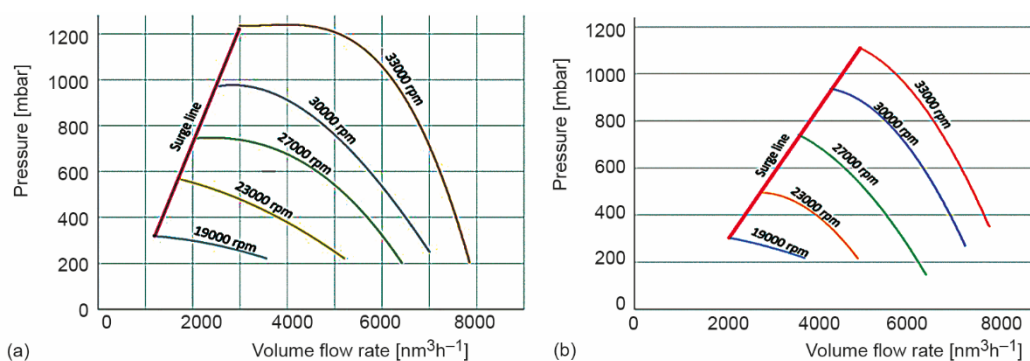


Figure 7. Performance map (a) original impeller and (b) thickened impeller

## Conclusion

In terms of the structural integrity of the thickened impeller, there is an overall improvement to its structural strength. The thickened impeller is demonstrated to endure the mechanical and fluid stresses acting upon it. However, the performance of the machine is impacted by the impellers. The volume flow capacity is reduced compared to the original impeller, potentially attributable to a slight decrease in volume flow arising from the augmented blade thickness.

The stress encountered by the original impeller after the FSI analysis was 577.95 MPa, which surpasses the ultimate tensile stress of the impeller material (AL 7075 T6) that possesses a ultimate tensile stress of 493.8 MPa. When the impeller blade thickness was increased by 0.1 mm, the Von Mises stress was 208.47 MPa.

According to the CFD results, the thickened impeller polytropic efficiency increased to 86.57%, compared to the original impeller polytropic efficiency of 75.8%. When the thickened impeller was employed, the volumetric flow declined from 4211.3 m<sup>3</sup>/h to 3658.3 m<sup>3</sup>/h. Based on the obtained data, it was determined that augmenting blade thickness reduces the stresses exerted upon the blade.

The polytropic efficiency was proven to be enhanced, as well as the mass-flow rate, which exhibited insignificant changes. Consequently, from this study, it may be concluded that augmenting the impeller thickness had an overall positive effect, as it can operate under the same conditions as the older impeller with minimal effects on the overall performance [16]. By utilizing CFD software, the required time and cost of manufacturing and testing all six different impellers were minimized and future impellers can be manufactured more optimally. The finite element method in COMSOL Multiphysics and the finite volume method in ANSYS CFX are used in the literature to ensure that the numerical predictions as well as the basic CFD equations are appropriate for the solution [3, 17]. Comparative analyses are planned for future studies to simulate engineering problems.

## Acknowledgment

We would like to acknowledge the funding provided by HAUS Centrifuge Technologies and for providing the testing facilities for this case study. We would also like to acknowledge Aydin Adnan University for their support.

## Nomenclature

$Q$  – volume flow rate, [m<sup>3</sup>s<sup>-1</sup>]

$P1$  – inlet pressure, [bar]

$P2$  – discharge pressure, [bar]

$T1$  – inlet temperature, [°C]

$T2$  – discharge temperature, [°C]

### Greek symbols

$\eta$  – polytropic exponent

$\eta_p$  – polytropic efficiency, [%]

### Acronyms

FSI – fluid-solid interaction

CAE – computer aided engineering

ISO – International Organization of Standardization

## References

- [1] Baolong, G., et al., Study on Application on CAE in a Centrifugal Compressor Impeller, *Advanced Materials Research*, 787 (2013), Sept., pp. 594-599
- [2] Berna, F. K., et al., A Comparison of One-Way and Two-Way Coupling Methods for Numerical Analysis of Fluid-Structure Interactions, *Journal of Applied Mathematics*, 2011, (2011), Nov., 853560
- [3] Ertugruk, I., et al., Analysis of Thermal Barrier Coated Pistons in the COMSOL and the Effects of their Use with Water + Ethanol Doped Biodiesel, *Thermal Science*, 26 (2022), 4A, pp. 2981-2989
- [4] Cui, B., et al., Influence of Cutting Angle of Blade Trailing Edge on Unsteady Flow in a Centrifugal Pump under Off-Design Conditions, *MDPI Applied Sciences*, 10 (2020), 2, 580
- [5] Lee, K., et al., The Evaluation of Aerodynamic Interaction of Wind Blade using Fluid Structure Interaction Method, *Journal of Clean Energy Technologies*, 3 (2015), 4, pp. 270-275
- [6] Zheng, X., et al., Effect of Temperature on the Strength of a Centrifugal Compressor Impeller for a Turbocharger, *Mechanical Engineering Science*, 227 (2012), 5, pp. 869-904
- [7] \*\*\*, International Standards ISO 5167 Measurement of Fluid Flow by Means of Pressure Differential Devices Inserted in Circular Cross-Section Conduits Running Full-Part 4: Venturi Tubes, (2003)
- [8] \*\*\*, International Standards ISO 5389 Turbo Compressor- Performance Test Code Second Edition, (2005)
- [9] Jebieshia, T. R., et al., Aerodynamic and Structural Characteristics of a Centrifugal Compressor Impeller, *Applied Sciences*, 9, (2019), 16, 3416
- [10] Hlaing, N. N., et al., Structural Analysis of Compressor Blades for Turbocharger by Using the Different Materials, *International Journal of Advances in Scientific Research and Engineering (IJASRE)*, 5 (2019), 12, pp. 2320-2092
- [11] Pei, J., et al., Dynamic Stress Analysis of Sewage Centrifugal Pump Impeller Based on Two-way Coupling Method, *Chinese Journal of Mechanical Engineering*, 27 (2014), 2, 369
- [12] Celtek, M. S., Engin, T., 3-D Numerical Investigation and Optimization of xCentrifugal Slurry Pump Using Computational Fluid Dynamics, *J. of Thermal Science and Technology*, 36 (2016), 1, pp. 69-83
- [13] Babalola, P. O., et al., Performance Evaluation of a Centrifugal Pump with different Impeller Materials, *Journal of Physics: Conference Series*, 1378 (2019), 2, pp. 1742-6596
- [14] Moorthy, C. H. V., et al., Computational Analysis of a CD Nozzle with 'SED' for a Rocket Air Ejector in Space Applications, *International Journal of Mechanical and Production Engineering Research and Development (IJMPERD)*, 7 (2017), 1, pp. 53-60
- [15] Xu, Z., et al., Effect of Blade Thickness on Internal Flow and Performance of a Plastic Centrifugal Pump, *Machines*, 10 (2022), 1, 61
- [16] Abood, M. H., et al., Stress Analysis of Centrifugal Fan Impellers, *Al-Rafidain Engineering Journal (AREJ)*, 20 (2012), 6, pp. 60-69
- [17] Liu, H., et al., A MEMS-Based Piezoelectric Cantilever Patterned with PZT thin Film Array for Harvesting Energy from Low Frequency Vibrations, MEMS Accelerometers: Design, Applications and Characterization, *Physics Procedia*, 13 (2022), 10, 1608